*Research Article*

# Machining Behavior of Al-MMC Reinforced with Hybrid Additives: Effects of Cutting Parameters – A Taguchi Approach

**Mohammad Hasanifard** [ID] **, Reza Azarafza**[*] [ID] **, Mohammad Hossein Alaei** [ID]

**, Moslem Najafi** [ID]

*Faculty of Materials and Manufacturing Technologies, Malek Ashtar University of Technology, Tehran, Iran*

## ARTICLE INFO

## ABSTRACT

Aluminum-based composites reinforced with $Mg_2Si$ particles are valued for their engineering properties. This study examines how cutting parameters and Ag, Bi, and Sr additives affect tool wear and surface roughness during both dry and wet turning of Al–$Mg_2Si$ composites. Using a Taguchi design, we varied spindle speed, feed rate, depth of cut, and lubrication to determine their relative impacts on tool wear area and surface roughness. Composites were fabricated through casting and examined using SEM–EDS techniques to assess microstructural characteristics and wear morphology. Feed rate emerged as the most critical factor, while wet machining with a biodegradable fluid markedly improved both tool life and finish. Among the materials tested, the composite containing all three additives delivered the lowest wear and finest surface. Specifically, the 14.47% improvement in dispersion uniformity was observed when all additives were used, while tool wear was reduced by 24.04%, and surface roughness improved by 18.94% under optimized machining conditions (spindle speed of 1000 rpm, feed rate of 0.12 mm/rev, and depth of cut of 1 mm). Regression modeling supported the experimental findings and demonstrated strong predictive accuracy. Confirmation trials under optimized conditions verified these trends. These results highlight the role of additive elements not only in modifying microstructure but also in enhancing machinability. The findings provide clear guidance on selecting additive combinations and machining settings to maximize productivity, extend tool life, and achieve superior surface integrity in Al–$Mg_2Si$ composite turning.

## 1. Introduction

In recent years, particulate-reinforced aluminum metal matrix composites (MMCs) have gained widespread use in the automobile and aerospace industries due to their low specific weight, enhanced wear resistance, reduced thermal expansion, and superior mechanical properties [1-4].

Although these composites are produced in near-net shape, additional secondary machining processes are often necessary to meet specific dimensional and surface finish requirements [5-7]. Industrial interest has driven extensive research into the machining of composite-based metals. However, the primary observation is that reinforcing the base metal with hard particles can complicate machining operations, resulting in

---

**Cite this article as:**

increased crater wear, inferior surface quality, and higher manufacturing costs. Most studies indicate that carbide and polycrystalline diamond (PCD) tools are predominantly used for machining MMCs [8-10]. Numerous studies suggest that carbide tools can serve as viable alternatives to CBN and PCD tools under specific conditions [9, 11, 12]. An essential step in maximizing efficiency and stability when machining metal-based composites is optimizing the machining parameters. Thus, the appropriate selection of these parameters is vital for developing a cost-effective machining process. However, there are relatively few studies reported on the turning process in this context [13-15].

Bharat and Bose [16] reviewed the machining behavior of metal matrix composites (MMCs) and showed that the inherent hardness and heterogeneity of reinforcements such as SiC, $B_4C$, and $Al_2O_3$ make machining considerably more difficult than for monolithic alloys. They emphasized that conventional processes, including turning, drilling, milling, and grinding, are strongly influenced by cutting parameters, which directly affect tool wear, surface integrity, and production cost. Their study also highlighted the role of optimization techniques such as Taguchi design, RSM, and ANN in improving machinability by balancing tool life and surface quality.

Bharat and Bose [17] further analyzed the machinability of AA7178 reinforced with SiC and $TiO_2$ nanoparticles using Taguchi and GRA methods. They found that feed rate strongly affects surface roughness, while cutting speed and depth of cut mainly influence cutting forces, confirming the reliability of Taguchi design for optimizing machining of MMCs.

Rodriguez et al. [18] highlighted the role of reinforcement in enhancing matrix hardness and improving the mechanical properties. Additionally, Palanikumar and Karthikeyan [19] observed that surface roughness is influenced by both the feed rate and the volume fraction of particles. Ozben et al. [20] examined the effect of different reinforcement ratios, 5, 10, and 15 wt% of ceramic particles, on the mechanical properties and machinability of composites, concluding that some mechanical properties had improved. Regarding the machinability of MMCs, most previous studies have focused on Al-SiC and Al-$Al_2O_3$ MMCs. Cast Al-$Mg_2$Si composites contain coarse primary $Mg_2$Si particles, which can negatively affect the composite's mechanical properties, particularly elongation and ductility. To achieve the desired mechanical properties, these particles must be modified. This modification can be accomplished by adding specific elements, such as silver (Ag), strontium (Sr), or bismuth (Bi) [21-23].

Understanding tool wear mechanisms is critical in the machining of metal matrix composites (MMCs), particularly Al-$Mg_2$Si-based systems, due to their inherent abrasiveness and heterogeneity. [24]. Tool wear not only influences dimensional accuracy and surface integrity but also directly affects process efficiency and tool life. Generally, tool wear in machining operations can occur through several mechanisms, including abrasive wear, adhesive wear, diffusion wear, and oxidation wear—each driven by different thermal and mechanical interactions at the tool-workpiece interface. [25, 26]. Identifying the dominant wear mechanism under specific machining conditions is essential for optimizing cutting parameters, selecting appropriate tool materials, and improving overall productivity. Moreover, minimizing tool wear through mechanism-based analysis contributes to reduced tooling costs, enhanced surface quality, and more sustainable manufacturing processes. [27, 28].

Despite the progress made, most previous works have primarily concentrated on the mechanical and microstructural properties of Al–$Mg_2$Si composites or on the role of conventional ceramic reinforcements such as SiC and $Al_2O_3$. Only a limited number of studies have addressed how modifying elements influence not only the microstructure but also the machinability of Al–$Mg_2$Si composites in terms of tool wear and surface finish. Moreover, the combined effect of these modifiers on machining performance has not been investigated. Therefore, this study aims to bridge this gap by examining the influence of Ag, Sr, and Bi additives, both individually and in combination, on the machinability of Al–$Mg_2$Si composites under various cutting parameters, with a particular focus on surface roughness and tool wear using a Taguchi design approach.

## 2. Experimental Procedure

### 2.1. Fabrication Of MMC Blocks

Composite material blocks were fabricated using the casting method, as depicted in Figure 1 and detailed in Table 1. A commercial Al-Si alloy (LM6), along with pure magnesium and pure aluminum, was used as a starting material to adjust the chemical composition. These materials were melted to produce an Al-15%$Mg_2$Si ingot. A 2-kg ingot was melted using a resistance furnace with a silicon carbide crucible, maintained at a temperature of 750 ± 5 ∘ C.

Three alloying elements, silver (Ag), bismuth (Bi), and strontium (Sr), in their pure metallic forms, were separately added to the melt as

modifying agents at 7 wt%, 1.5 wt%, and 2 wt%, respectively. Ag was used to improve thermal conductivity and accelerate solidification, promoting $Mg_2Si$ particle refinement. Sr was added to modify the microstructure, while Bi, due to its low melting point, enhanced melt homogenization and acted as a solidification-phase lubricant, thereby improving machinability [21, 22, 29]. The dissolution and homogenization processes were carried out over 15 minutes, during which the melt was stirred, and the surface was skimmed to remove impurities. The molten alloy was then poured into a cylindrical ceramic mold (outer diameter of 30 mm, height of 150 mm, and wall thickness of 10 mm), which had been preheated to 750 ∘ C for 15 minutes.

**Table 1.** The fabricated composite components.

| Composite No. | Composite components |
| --- | --- |
| 1 | Al-15%Mg₂Si |
| 2 | Al-15%Mg₂Si+7%Ag |
| 3 | Al-15%Mg₂Si+1.5%Bi |
| 4 | Al-15%Mg₂Si+2%Sr |
| 5 | Composition |
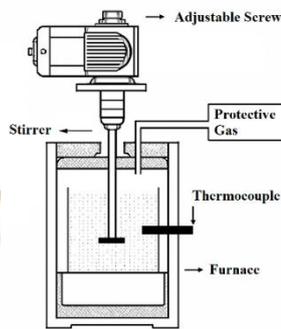


(a)



(b)                    (c)

**Figure 1.** (a) Schematic of the casting system employed; (b) Induction melting system; (c) Casting mold.

A small portion of the Al-Mg₂Si composite was sectioned, polished, and examined under a 400x optical microscope to assess particle distribution (Figure 2). Uniform homogeneity with slight particle agglomeration was observed. Quantitative analysis was performed at 25°C and 38% humidity (Table 2).
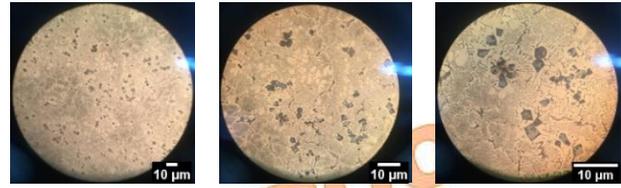


(a)                (b)                (c)

**Figure 2.** The etched surface of the Al-15%Mg₂Si composite at three magnifications: (a) 100x, (b) 200x, and (c) 400x.

## 2.2. Experimental Design

The cutting parameters used in this work are presented in Table 3. The experimental parameters were selected according to industrial recommendations by the cutting tool manufacturer. The MeC Green biofluid was used as the lubricant in the wet cutting conditions. To construct an efficient experimental plan with fewer experiments [30]the L16 Taguchi orthogonal array was used for each material. Given the large number of factors (spindle speed, feed rate, depth of cut, and lubrication) and levels involved, alternative methods such as full factorial or response surface methodology (RSM) would have required significantly more trials (256 trials for full factorial and higher-order models for RSM), which would not have been feasible in terms of time and resources. Furthermore, the Taguchi method is known for its accuracy in providing statistically reliable results even with a reduced number of experiments, while ensuring effectiveness in capturing the main effects of the parameters [17, 31, 32]. Accordingly, 80 tests (16 runs for each of the five composite types) were performed, and with the inclusion of repeated confirmation runs, a total of 160 machining tests were conducted. The average of the repeated measurements was considered as the final output for both surface roughness and tool wear, thereby ensuring repeatability and statistical reliability of the results.

**Table 3.** Experimental parameters utilized.

| Cutting Parameters | Levels | | | |
| --- | --- | --- | --- | --- |
| Spindle Speed (rpm) | 360 | 500 | 710 | 1000 |
| Feed Rate (mm/rev) | 0.08 | 0.12 | 0.2 | 0.28 |
| Depth of Cut (mm) | 0.5 | 1 | 1.5 | 2 |
| Cooling conditions | Dry | Wet | - | - |

**Table 2.** Chemical composition of fabricated composites.

| Materials | Al | Mg | Si | Fe | Cu | Mn | Zn | Cr |
|---|---|---|---|---|---|---|---|---|
| Al-15%Mg$_2$Si | Base | 9.53 | 5.61 | 0.21 | 0.17 | 0.12 | 0.13 | 0.01 |
| Al-15%Mg$_2$Si + 7%Ag | Base | 9.12 | 5.66 | 0.17 | 0.01 | 0.08 | 0.09 | 0.02 |
| Al-15%Mg$_2$Si + 1.5%Bi | Base | 9.40 | 5.43 | 0.16 | 0.12 | 0.15 | 0.14 | 0.02 |
| Al-15%Mg$_2$Si +2%Sr | Base | 9.92 | 4.97 | 0.32 | 0.24 | 0.10 | 0.17 | 0.07 |
| Composition | Base | 8.78 | 4.95 | 0.14 | 0.11 | 0.13 | 0.15 | 0.03 |

### 2.3. Machining Trials

The lathe used in these experiments was an SN71C model, manufactured by Tos Machine Tools in Czechoslovakia. The cutting tool employed in this study is a cemented carbide tool coated with tungsten carbide, sourced from Bohlerit, Austria, and selected according to the ISO 3685:1993 standard. The geometry of the tools is square-shaped, and they are commercially designated as CNMG-120408-MS under the ISO standard. Their serial number, based on the manufacturer's coding system, is LC415Z(HC-S15). This grade is a coated tool with tungsten carbide coating, equipped with a chip breaker, and offers high wear resistance. The tool holder used was MCLNR2020K12, in accordance with ISO standards. The setup for conducting the experiments in both dry and wet conditions is illustrated in Figure 3. The physical properties of the composites and their positioning in the lathe are presented in Table 4. To measure the surface roughness of the machined in-situ Al-Mg$_2$Si composite, a Mitutoyo SJ-201 surface roughness tester, manufactured in Japan, was used. The measurement was conducted according to the ISO 4287 standard, employing the Ra surface roughness criterion [33].

A Vega2 scanning electron microscope (SEM), manufactured by Tescan (Czech Republic), was used to examine the fabricated composites and the tool wear surfaces produced under different machining parameters. Mapping and EDS analyses were then applied to areas of interest and regions suspected of changing. Additionally, the wear mechanism was identified based on the wear morphology observed on the tool surface, and the corresponding wear area was quantitatively measured using ImageJ software.
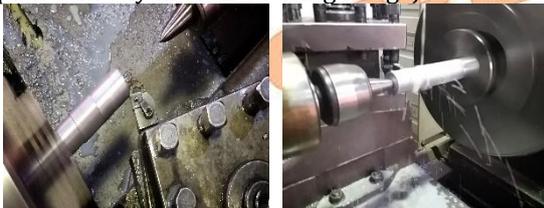


(a)                              (b)

**Figure 3.** The setup for conducting the experiments in both (a) Dry and (b) Wet conditions.

**Table 4.** The physical properties of the composites and their positioning in the lathe.

| Parameter | Value (mm) |
|---|---|
| Workpiece length | 150 |
| Workpiece diameter | 30 |
| Machined length in each experiment | 18 |
| Workpiece chuck engagement length | 30 |

## 3. Results And Discussion

### 3.1. Fabricated Composites

Figure 4 shows the SE image and mapping analysis of the etched surface of the composite fabricated with all modifier elements. It was observed that Mg$_2$Si particles were homogeneously distributed within the aluminum matrix. Strontium particles tended to position themselves around the ceramic Mg$_2$Si particles, while silver and bismuth particles were uniformly dispersed throughout the matrix. The tendency of strontium particles to position themselves around Mg$_2$Si particles was likely due to their high reactivity with Mg$_2$Si during the composite's solidification process. This interaction promoted the formation of interfacial bonds, leading strontium to concentrate near the Mg$_2$Si particles. This behavior enhanced the overall structural integrity at the particle-matrix interface, ultimately contributing to a more stable composite microstructure [34].

The even distribution of silver and bismuth particles throughout the aluminum matrix resulted from their lower affinity for interaction with Mg$_2$Si particles. This characteristic prevented clustering around specific phases, promoting a uniform dispersion within the aluminum matrix and contributing to balanced enhancements in the composite's properties.

While mapping analysis suggested good dispersion of the additive elements, a quantitative measure of dispersion uniformity was carried out using ImageJ software. The Homogeneity Index for unreinforced composites was 0.76, while for the composites reinforced with all additive elements, it increased to 0.87, indicating an improvement of approximately 14.47% in dispersion uniformity.

As illustrated in Figure 4, the uniform distribution of Mg$_2$Si particles demonstrates the refinement effect induced by Sr and the lubricating role of Bi. These microstructural features directly contribute to the reduction in tool wear, which is consistent with the findings of Wu et al. [35] and Farahany et al. [34].
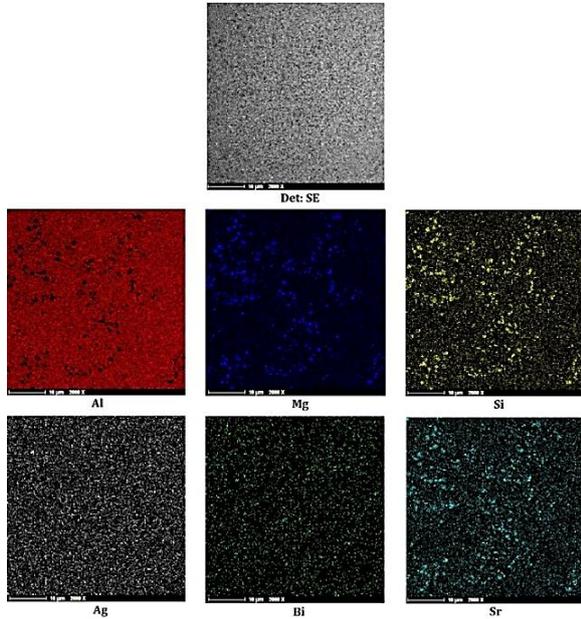


**Figure 4.** SE image and mapping analysis of the composite fabricated with all modifier elements.

### 3.2. Surface Roughness

Surface roughness was measured according to the ISO 4287 standard, with the Ra parameter recorded using a roughness tester after each machining step. To ensure the reliability of the results, six roughness measurements were taken from different areas of each machined surface. In each measurement, five segments of 0.8 mm (a total of 4 mm) were carefully analyzed. The final surface roughness results, along with the experimental design matrix, are presented in Table 5.

Taguchi analysis was performed on the obtained results. Four input parameters were examined both individually and in combination to evaluate their influence on the output response. The R-square value reflects the model's ability to represent the experimental data; higher values indicate a stronger correlation and a more reliable prediction of the response behavior. Figure 5 illustrates the mean surface roughness for different machining parameters, while Table 6 presents the results of the Taguchi analysis for mean surface roughness based on the machining parameters.
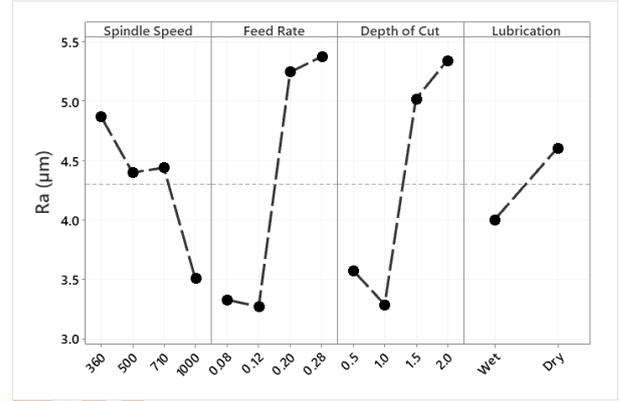


**Figure 5.** The mean surface roughness for different machining parameters.

**Table 6.** The surface roughness results along with the contribution of each parameter.

| Level | Spindle Speed | Feed Rate | Depth of Cut | Lubrication |
|---|---|---|---|---|
| 1 | 4.870 | 3.325 | 3.570 | 4.003 |
| 2 | 4.400 | 3.268 | 3.285 | 4.606 |
| 3 | 4.440 | 5.247 | 5.020 | |
| 4 | 3.508 | 5.377 | 5.342 | |
| Delta | 1.362 | 2.110 | 2.057 | 0.604 |
| Rank | 3 | 1 | 2 | 4 |
| R-square | 97.41% | | | |
| Adjusted R-square | 92.22% | | | |

Based on the high R-square value of 97.41%, it was concluded that the selected parameters and their levels effectively explain the variations in the dependent variable, which is surface roughness. Additionally, the adjusted R-square value of 92.22% confirms that the independent variables continue to provide a good explanation of the variations, even with the model's increased complexity.

**Table 5.** The L16 orthogonal array from the design of experiments was utilized for each tested MMC.

| Test No. | Machining Parameters | | | | Results |
| | Lubrication Method | Depth of Cut (mm) | Feed Rate (mm/rev) | Spindle Speed (rpm) | Ra (μm) |
| --- | --- | --- | --- | --- | --- |
| 1 | Wet | 0.5 | 0.8 | 360 | 2.53 |
| 2 | Wet | 1 | 0.12 | 360 | 2.71 |
| 3 | Dry | 1.5 | 0.2 | 360 | 6.63 |
| 4 | Dry | 2 | 0.28 | 360 | 7.61 |
| 5 | Dry | 1 | 0.8 | 500 | 2.76 |
| 6 | Dry | 0.5 | 0.12 | 500 | 3 |
| 7 | Wet | 2 | 0.2 | 500 | 6.29 |
| 8 | Wet | 1.5 | 0.28 | 500 | 5.55 |
| 9 | Wet | 1.5 | 0.8 | 710 | 4.34 |
| 10 | Wet | 2 | 0.12 | 710 | 3.8 |
| 11 | Dry | 0.5 | 0.2 | 710 | 5.01 |
| 12 | Dry | 1 | 0.28 | 710 | 4.61 |
| 13 | Dry | 2 | 0.8 | 1000 | 3.67 |
| 14 | Dry | 1.5 | 0.12 | 1000 | 3.56 |
| 15 | Wet | 1 | 0.2 | 1000 | 3.06 |
| 16 | Wet | 0.5 | 0.28 | 1000 | 3.74 |

Taguchi analysis revealed that feed rate had the most significant impact on surface roughness, as evidenced by the highest delta value (2.110). The results, illustrated in Figure 5, show a pronounced increase in surface roughness beyond a feed rate of 0.12 mm/rev, indicating the composite's sensitivity to higher feed rates. This behavior is attributed to the composite's material characteristics—namely, the high thermal conductivity of aluminum and the flammability of magnesium—which facilitate efficient heat dissipation at moderate feed rates. However, feed rates below 0.12 mm/rev may lead to excessive polishing and insufficient chip removal, causing localized heat accumulation. This, in turn, can induce plastic deformation in the composite, particularly within the $Mg_2Si$ reinforcing phase, due to its ceramic nature and increased brittleness under thermal stress [11, 36].

The second most influential parameter on surface roughness is the depth of cut, which ranks just below feed rate with a delta value of 2.057. Based on the interpretation of Figure 5 and the four selected levels for this parameter, it was determined that the greatest slope (change) occurs between depths of 1 and 1.5 mm, with a depth of 1 mm resulting in the lowest surface roughness. Higher depths of cut lead to increased tool contact with the composite and the reinforcing particles, which results in greater wear and an increase in the cutting zone temperature, ultimately reducing surface quality [37]. Conversely, a depth of cut below 1 mm causes increased temperature in the cutting area due to greater surface contact between the tool and the $Mg_2Si$ ceramic-reinforced composite [38], placing it only slightly above the higher depths of cut in terms of surface roughness.

The third most influential parameter is the spindle speed, with a delta value of 1.362, placing

it significantly lower than the previous two parameters. As indicated by the gentler slope in Figure 5, its impact on surface roughness is considerably less. However, within the four levels analyzed, two major changes in surface roughness were observed: one between 360 and 500 rpm and another between 710 and 1000 rpm, where a significant improvement in surface roughness was detected. The principle that increasing cutting speed leads to a more effective contact between the tool and the workpiece (domination of tool material over workpiece material) is inevitable. This results in a reduced final depth of cut due to more uniform cuts, decreased thermal stresses due to more even heat distribution, and reduced friction due to less likelihood of built-up edge formation [39], as observed in this study.

The optimal speed for achieving the desired surface quality was identified as 1000 rpm. Reducing the spindle speed below this level negated the mentioned mechanisms, leading to excessive heat generation in the cutting area, which in turn caused built-up edge formation, plastic deformation of the composite surface, and an increase in roughness. On the other hand, exceeding this spindle speed moves the process beyond conventional turning towards polishing, which follows different principles and is not covered in this study.

It is essential to note that increasing spindle speed must be done with caution, as excessively high speeds can lead to issues such as accelerated tool wear, increased heat generation, and even reduced surface quality [40]. In this study, no behavior indicating a decrease in surface quality due to increased cutting speed, which would suggest a temperature rise [41] in the cutting area, was observed. Thus, it was concluded that

within the selected spindle speed range, excessive temperature increases did not occur.

The fourth and least influential parameter is lubrication, which compares two machining conditions: dry and wet. With a delta value of 0.604, it is ranked significantly lower than the other parameters. Based on Figure 5 and the slope between these two conditions, it was concluded that using cutting fluid significantly enhances surface quality. This improvement is due to the cutting fluid's ability to prevent excessive heat generation by reducing friction between the tool and the composite, decreasing pressure, wear, and corrosion, and improving tool movement through its lubricating effect. Additionally, the cutting fluid helps prevent the formation of surface defects by removing chips from the cutting area and regulating the temperature through its heat transfer capabilities [42].

During the machining of $Mg_2Si$ particle-reinforced composites, high surface roughness was observed. One of the primary reasons for this is the high hardness and wear resistance of the reinforcing particles, such as $Mg_2Si$. This high hardness means that these particles offer significant resistance to cutting during machining, leading to increased tool wear and surface roughness on the workpiece [43]. Another contributing factor is the effect of heat and cutting phenomena during the machining of reinforced composites. The generated heat can alter the material properties and cutting behavior. Elevated temperatures can cause temporary melting or softening of the matrix and reinforcing particles, which in turn can lead to an increase in surface roughness [44]. Finally, the breaking or fracturing of reinforcing particles during machining can result in additional voids and irregularities on the surface of the workpiece, further contributing to increased surface roughness [45].

These findings are in agreement with Davim [46] and Palanikumar [19], who also identified feed rate as the most critical factor influencing surface finish in MMC turning. Similarly, Ozben et al. [20] observed that higher reinforcement ratios increased surface roughness, consistent with the effect of hard $Mg_2Si$ particles in our composites.

Using the predictive capability of the Taguchi results in Minitab software, optimal levels for all machining input parameters were determined, as shown in Table 7. Subsequently, the predicted values for average surface roughness and the signal-to-noise ratio were calculated. These predictions were compared with experimental results obtained using the optimal parameters, and the outcomes of this comparison are presented in Table 8.

**Table 7.** Optimal levels for each machining parameter for reducing surface roughness.

| Lubrication Method | Spindle Speed (rpm) | Depth of Cut (mm) | Feed Rate (mm/rev) |
|---|---|---|---|
| Wet | 1000 | 1 | 0.12 |

**Table 8.** Comparison of surface roughness: Statistical predictions vs. experimental data.

| Error% | Experimental | Statistical | |
|---|---|---|---|
| | Ra (μm) | Ra (μm) | S/N Ratio |
| 5.45 | 1.09 | 1.14938 | -6.25086 |

As expected, the selection of optimal values for the extracted machining parameters led to a significant improvement in surface roughness of the Al-$Mg_2Si$ composite. The average surface roughness index reached 1.14938 micrometers, indicating an acceptable surface quality, even approaching a polished finish. The low percentage error between the statistical and experimental methods demonstrates the high validity of the obtained results.

Based on the obtained results and their validation, a regression model was developed to predict surface roughness using feed rate, depth of cut, and rotational speed as input parameters. Equation 1 presents the regression model for estimating the surface roughness index of the Al-$Mg_2Si$ composite. Figure 6 shows the normal probability plot of the fitted regression model.

$$Ra = 1.720 - 0.001932(Spindle\ Speed) + 12.13(Feed\ Rate) + 1.410(Depth\ of\ Cut) \quad (1)$$
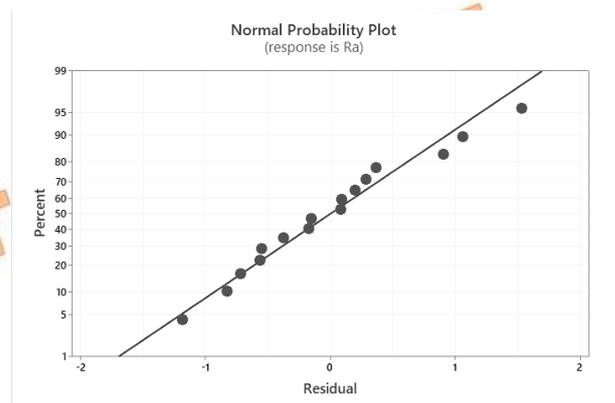


**Figure 6.** Normal probability plot for the fitted surface roughness model.

Based on Figure 6, in assessing the normal distribution of the data, it was inferred that the points are close to the straight line, indicating that the data follow a normal distribution [47]. Consequently, the fitted model in Equation 1 holds significant statistical importance in

predicting the surface roughness index of the Al-Mg$_2$Si composite.

Figure 7 illustrates the effect of different additives on the produced composite, as well as the composition of all additives, on the surface roughness relative to the test number.
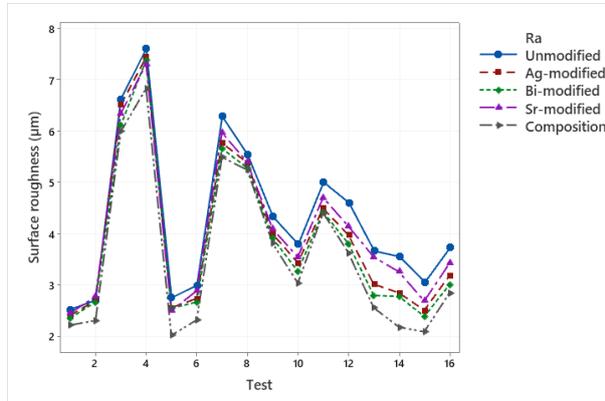


**Figure 7.** The impact of additive elements on the surface roughness of the Al-Mg$_2$Si composite.

The composite with bismuth exhibited the lowest surface roughness, followed sequentially by those with silver, strontium, and, lastly, the composite without any modifiers. In its optimized form, the composite incorporating all the mentioned additive elements demonstrated improved surface roughness. The addition of silver, bismuth, and strontium particles as reinforcing elements in the Al-Mg$_2$Si composite led to a reduction in surface roughness due to their ability to modify the microstructure and improve machinability.

Bismuth, being a low-melting-point element, acted as a solid lubricant during machining, reducing friction between the tool and the composite surface. [35]. This lubrication effect helped to minimize tool wear and thermal stress, leading to a smoother machined surface.

The reduction in final surface roughness observed in the Al-Mg$_2$Si composite with silver incorporation was primarily attributed to its enhanced thermal conductivity and lower melting point. These properties facilitated better heat dissipation during machining, which reduced thermal stress on the material and the cutting tool [48]. Additionally, silver acted as a lubricant, minimizing friction between the cutting tool and workpiece [49]. This combination of improved thermal management and reduced friction resulted in smoother cutting

action and better filling of surface irregularities, ultimately contributing to a finer surface finish.

Strontium, on the other hand, refined the microstructure by modifying the morphology of Mg$_2$Si particles, making them more uniformly distributed and smaller in size [34]. This uniform distribution reduced the occurrence of hard spots during cutting, resulting in a more consistent machining process and thus a lower surface roughness. As a result, the presence of these additive elements improved the overall surface quality of the Al-Mg$_2$Si composite by reducing the variation and resistance during the machining process.

### 3.3. Tool Wear

Based on ISO 3685, SEM and EDS analyses were used to investigate tool wear mechanisms and measure the wear area. BSE imaging enabled the identification of adhesive, abrasive, and oxidative wear zones through contrast variations. EDS confirmed material transfer from the workpiece to the tool. The wear area was quantified using ImageJ to support tool life assessment and machining parameter optimization.

As shown in Figure 8, SEM analysis revealed features characteristic of adhesive wear mechanisms, reflecting the influence of machining parameters on tool surface degradation and failure during cutting. The dominant wear mechanism during the turning of Al-Mg$_2$Si composites was adhesive wear, manifested as built-up edge (BUE) and built-up layer (BUL) on the tool rake surface. This behavior resulted mainly from intense tool–workpiece interaction combined with thermal and mechanical fluctuations in the cutting zone [50].

Figure 9 shows adhesive wear in the turning of Al-Mg$_2$Si composites, evident as built-up edge (BUE) on the tool rake surface. SE and BSE images highlight the worn region, while EDS confirmed the adhesion of workpiece material, which affected the tool surface and machining performance.

Figure 10 illustrates the variation in average tool wear area with changes in machining parameters, showing clear trends and identifying conditions of maximum and minimum wear. These results are supported by the Taguchi analysis in Table 9.
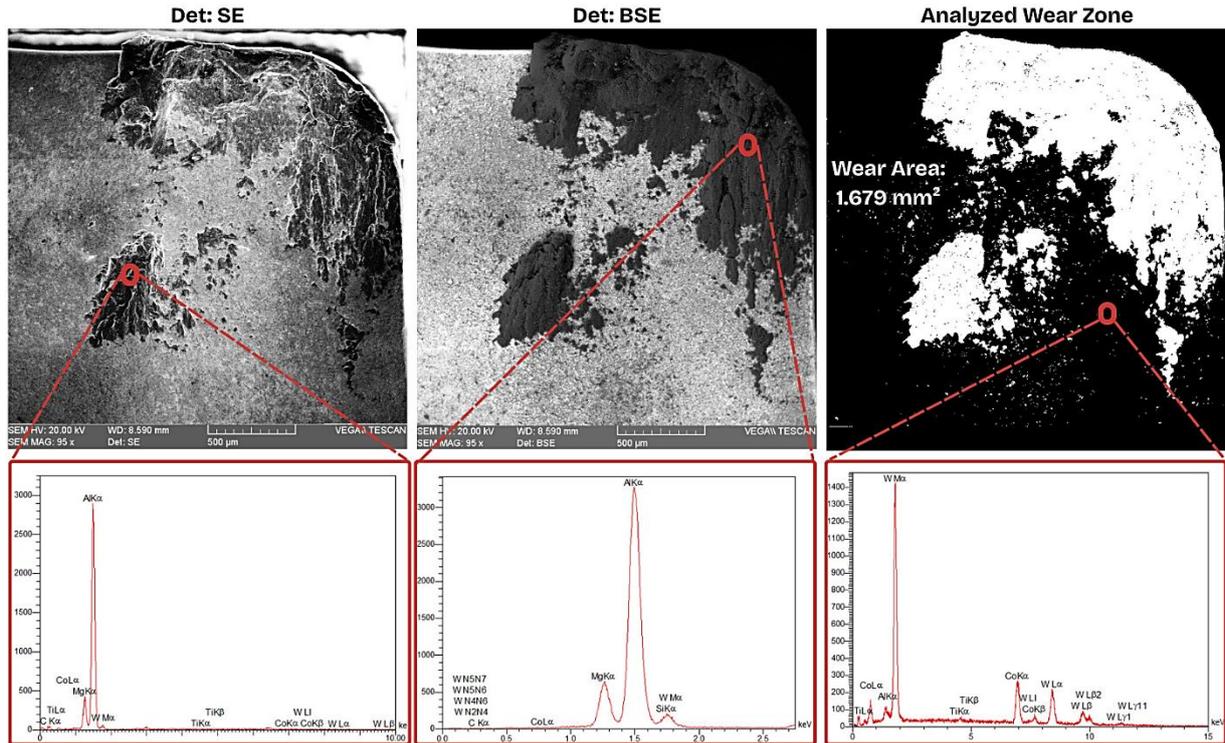
**Figure 8.** Tool wear mechanisms under machining conditions: L = dry, f = 0.2 mm/rev, d = 1.5 mm, N = 1000 rpm.
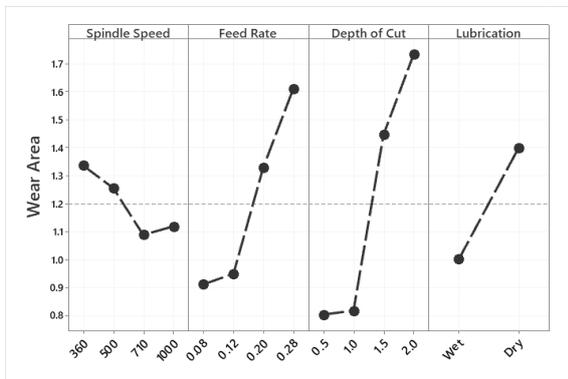


**Figure 10.** The mean tool wear area for different machining parameters.

In the first stage, the coefficient of determination ($R^2$) was calculated as 96.03%, indicating a strong correlation between tool wear and the machining parameters. The adjusted $R^2$ value of 88.10% further confirmed the model's validity by accounting for its complexity, suggesting that the selected parameters had a statistically significant and meaningful effect on tool wear.

**Table 9.** The surface roughness results along with the contribution of each parameter.

| Level | Spindle Speed | Feed Rate | Depth of Cut | Lubrication |
|---|---|---|---|---|
| 1 | 1.3365 | 0.9110 | 0.8022 | 1.0010 |
| 2 | 1.2560 | 0.9490 | 0.8165 | 1.3986 |
| 3 | 1.0882 | 1.3298 | 1.4470 | |
| 4 | 1.1185 | 1.6095 | 1.7335 | |
| Delta | 0.2483 | 0.6985 | 0.9313 | 0.3976 |
| Rank | 4 | 2 | 1 | 3 |
| R-square | 96.03% | | | |
| Adjusted R-square | 88.10% | | | |

Statistical analysis identified depth of cut as the most influential factor on tool wear, with a delta value of 0.9313. As shown in Figure 10, tool wear remained nearly constant from 0.5 mm to 1 mm but increased sharply beyond 1 mm. This rise is attributed to higher mechanical stresses and cutting forces, leading to elevated temperatures at the tool–workpiece interface, promoting adhesive wear mechanisms such as BUE and BUL formation [28]. Additionally, greater interaction with hard $Mg_2Si$ particles intensified abrasive wear [51].
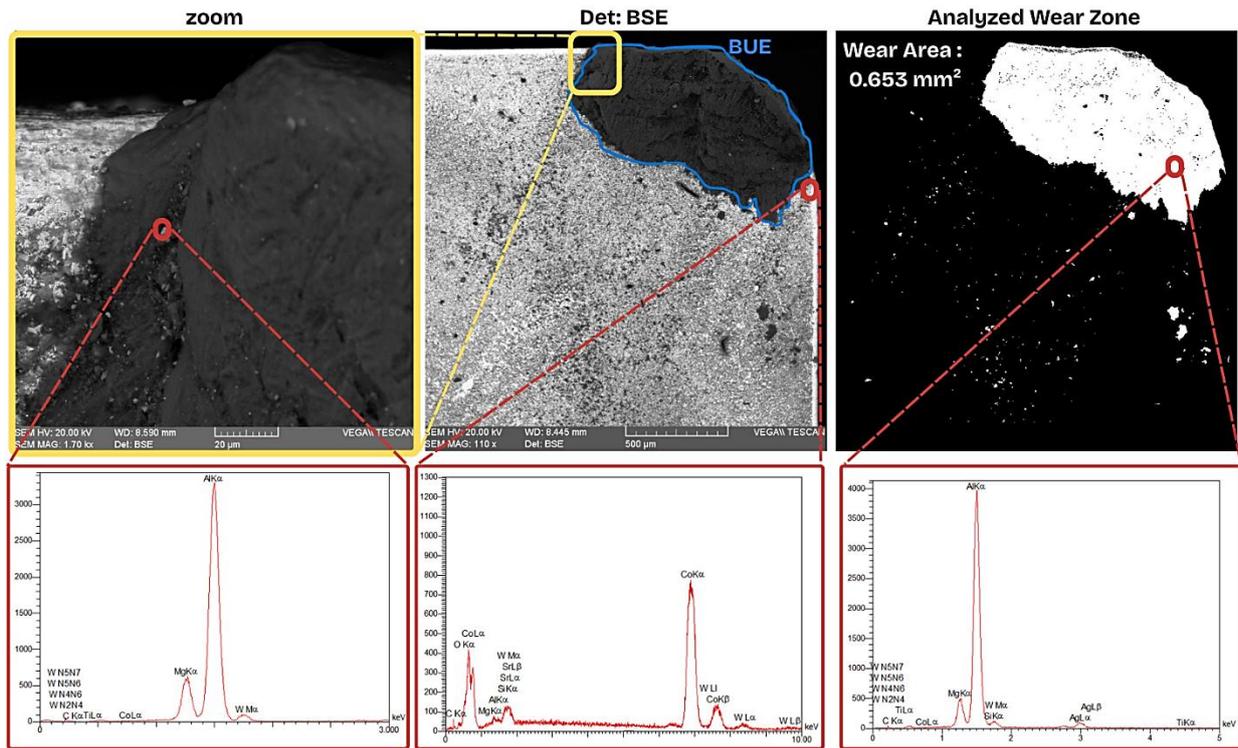
**Figure 9.** Tool wear mechanism under machining conditions: L = wet, f = 0.2 mm/rev, d = 1 mm, N = 1000 rpm.

Feed rate was identified as the second most influential factor on tool wear, with a delta value of 0.6985. As shown in Figure 10, tool wear remained relatively stable up to 0.12 mm/rev but increased significantly at higher feed rates of 0.2 and 0.28 mm/rev. This increase is attributed to higher shear forces and localized temperatures at the tool–workpiece interface [52, 53]. At lower feed rates, adhesive wear dominated due to longer tool–material interaction, whereas higher feed rates intensified abrasive wear mechanisms through increased fragmentation of $Mg_2Si$ particles and higher contact stresses [54, 55].

Lubrication strategy ranked third in influencing tool wear, with a delta value of 0.3976. As illustrated in Figure 10, the use of a biodegradable cutting fluid significantly reduced the wear area compared to dry machining. This reduction is attributed to lower friction, improved heat dissipation, and more effective chip evacuation [56]. These factors collectively decreased adhesive wear and prevented chip accumulation on the tool surface.

Spindle speed was identified as the least influential parameter on tool wear, with a delta value of 0.2483. As shown in Figure 10, increasing the speed from 360 to 710 rpm reduced wear due to lower cutting forces and more uniform heat distribution [57]. However, further increase to 1000 rpm led to a relative rise in wear, likely due to higher temperatures and the formation of unstable built-up layers. These findings suggest

that an optimal speed around 710 rpm, combined with effective lubrication and coated tools, can help minimize wear and improve machining outcomes.

The predominance of adhesive wear mechanisms observed in this study is consistent with the results of Ciftci [25] and Laghari et al. [24], who reported built-up edge formation as the main wear feature in MMC turning. The beneficial effect of wet machining also aligns with Bertolini et al. [50] and Singh et al. [56].

In Table 10, the optimal machining parameters were identified to minimize tool wear while maintaining process efficiency. The predicted values for average tool wear area and signal-to-noise (S/N) ratio were calculated using the Taguchi model. Confirmation experiments under optimized conditions were conducted, and the results, shown in Table 11, were compared with the predicted values. The close agreement between experimental and predicted data confirmed the accuracy and effectiveness of the Taguchi model in determining optimal machining conditions.

**Table 10**. Optimal levels for each machining parameter for reducing tool wear.

| Lubrication Method | Spindle Speed (rpm) | Depth of Cut (mm) | Feed Rate (mm/rev) |
|---|---|---|---|
| Wet | 710 | 0.5 | 0.08 |

**Table 11.** Comparison of tool wear results: Statistical predictions vs. experimental data.

| Error% | Experimental | Statistical | |
|---|---|---|---|
| | Wear Area (mm$^2$) | Wear Area (mm$^2$) | S/N Ratio |
| 7.85 | 0.219 | 0.203063 | 6.60033 |

The minimal difference in tool wear between the conditions of 1 mm cutting depth and 0.12 mm/rev feed rate, compared to the optimal settings, indicates that increasing these parameters can enhance machining efficiency without significantly affecting wear. This offers a practical solution for improving productivity and reducing machining time when tool wear is not the primary concern.

Equation 2 represents the final regression model for tool wear in Al-Mg$_2$Si machining. The model identifies the most influential parameters on wear and their impact on the process. It serves as a tool for optimizing machining conditions, improving wear prediction, reducing tool replacement costs, and enhancing efficiency [58].

$$Wear\ Area = -0.255-0.000358(Spindle\ Speed)+3.708(Feed\ Rate)+0.6848(Depth\ of\ Cut) \quad Wet$$

$$(2)$$

$$Wear\ Area = 0.142-0.000358(Spindle\ Speed)+3.708(Feed\ Rate)+0.6848(Depth\ of\ Cut) \quad Dry$$

Figure 11 shows the normal probability plot, confirming that the model fits the data well, with residuals following a normal distribution. The absence of significant outliers further supports the model's reliability and predictive accuracy, making it an effective tool for optimizing machining parameters and reducing tool wear.
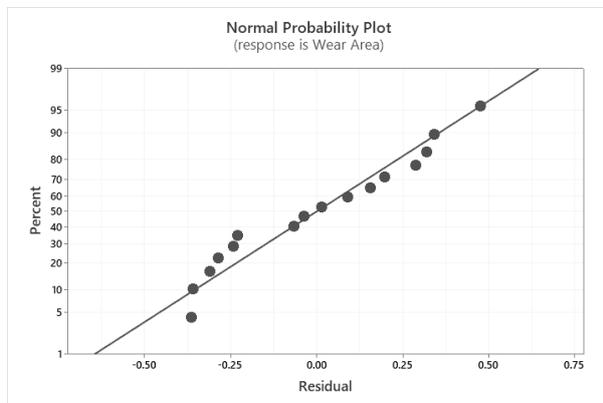


**Figure 11.** Normal probability plot for the fitted wear area model.

Figure 12 shows the impact of different additives on tool wear. Certain additives significantly reduced wear, while others increased it, depending on their physical and mechanical properties. Optimized additive combinations led to the lowest tool wear, highlighting the importance of selecting the right additives to improve tool performance and reduce replacement costs.
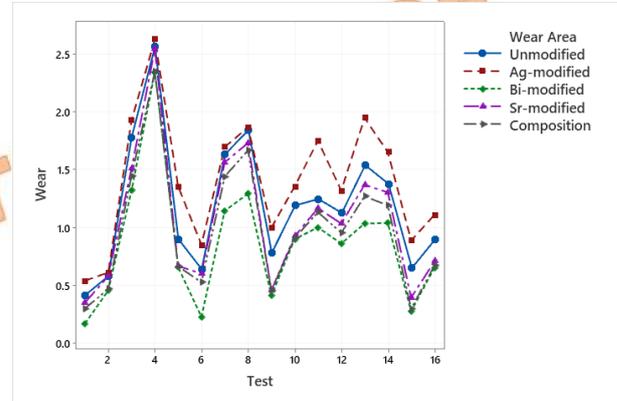


**Figure 12.** The impact of additive elements on the tool wear area.

The highest wear was observed in Ag-reinforced composites due to increased phase hardness and more severe wear mechanisms. The unreinforced composite showed the second-highest wear, indicating the notable influence of the base alloy's mechanical properties on tool degradation.

Sr- and Bi-reinforced composites exhibited reduced tool wear as a result of improved microstructure and better particle distribution. Among them, Bi had a stronger effect in minimizing wear by reducing adhesion and enhancing surface conditions during cutting.

The composite containing all additive elements resulted in the lowest tool wear, which was attributed to uniform particle dispersion and improved toughness [13, 59]. These findings confirmed that an optimized combination of reinforcing elements effectively reduced tool wear and enhanced machining performance.

Despite careful control of experimental conditions, several potential sources of error and limitations should be considered. These include slight variations in repeatability due to setup or operator handling, tool wear progression that may have affected consistency over the course of the experiments, and measurement variability, which was minimized by averaging multiple readings for surface roughness and tool wear. These considerations have been carefully addressed through experimental design, tool monitoring, and precise measurement techniques.

## 4. Conclusions

In this study, the effects of cutting parameters and Ag, Bi, and Sr additives on tool wear and surface integrity during the turning of Al–Mg₂Si composites were systematically investigated. Based on the experimental and statistical analyses, the following conclusions are drawn:

1. Parameter Influence: Feed rate had the greatest impact on both tool wear area and surface roughness, followed by depth of cut, lubrication strategy, and spindle speed.

2. Lubrication Benefit: Wet machining with a biodegradable cutting fluid substantially reduced wear and improved surface finish compared to dry conditions.

3. Additive Synergy: The composite containing the combined Ag–Bi–Sr additives exhibited the lowest tool wear and finest surface quality, owing to enhanced microstructural refinement, thermal management, and lubrication effects. Specifically, the 14.47% improvement in dispersion uniformity and 24.04% reduction in tool wear, along with an 18.94% improvement in surface roughness, were observed under optimized machining conditions.

4. The optimal machining parameters for improving tool life and surface integrity in the turning of Al–Mg₂Si composites are identified as follows: a spindle speed of 1000 rpm, a feed rate of 0.12 mm/rev, and a depth of cut of 1 mm, using wet machining with a biodegradable cutting fluid. These settings provide the best balance between tool wear and surface finish.

5. Model Validation: Taguchi and regression models demonstrated strong predictive capability ($R^2 > 96\%$), with confirmation tests under optimal conditions yielding errors below 8%.

6. Practical Guidance: The optimal machining settings (wet turning, moderate speed, low feed rate, shallow depth of cut) and additive selection identified here provide a validated framework for extending tool life, reducing costs, and achieving superior surface integrity in the machining of Al–Mg₂Si composites.

These findings offer actionable insights for manufacturing practitioners and establish a basis for future work on optimizing cutting tool materials and coolants for advanced metal–matrix composites.

Future studies could investigate the effect of varying concentrations of Ag, Bi, and Sr on the machinability of Al–Mg₂Si composites, which could provide a deeper understanding of how alloying element percentages influence tool wear and surface finish under different machining conditions. Additionally, X-ray diffraction (XRD) and other advanced characterization methods like SEM–EDS or TEM could be used to explore microstructural changes and the formation of intermetallic phases due to these alloying elements.

## Nomenclature

| | |
|---|---|
| *Ag* | Silver |
| *Al* | Aluminum |
| *Bi* | Bismuth |
| BSE | Backscattered Electrons |
| Det | Detector |
| EDS | Energy Dispersive X-ray Spectroscopy |
| Mg₂Si | Magnesium Silicide |
| MMC | Metal Matrix Composite |
| SEM | Scanning Electron Microscope |
| *SE* | Secondary Electrons |

## Funding Statement

## Conflicts Of Interest

The author declares that there is no conflict of interest regarding the publication of this article.

## References

[1] Emamy, M., Khorshidi, R. & Raouf, A.H., 2011. The influence of pure Na on the microstructure and tensile properties of Al-Mg2Si metal matrix composite. *Materials Science and Engineering: A, 528* (13-14), pp.4337-4342.

[2] Hadian, R., Emamy, M., Varahram, N. & Nemati, N., 2008. The effect of li on the tensile properties of cast Al–Mg2Si metal matrix composite. *Materials Science and Engineering: A, 490* (1-2), pp.250-257.

[3] Monaghan, J. & Brazil, D., 1998. Modelling the flow processes of a particle reinforced metal matrix composite during machining. *Composites Part A: Applied Science and Manufacturing, 29* (1-2), pp.87-99.

[4] Bharat, N. & Bose, P., 2023. Microstructure, texture, and mechanical properties analysis of novel aa7178/sic nanocomposites. *Ceramics International, 49* (12), pp.20637-20650.

[5] Igwe, N.C. & Ozoegwu, C.G., 2024. Analyzing empirically and optimizing surface roughness and tool wear during turning aluminum matrix/rice husk ash (rha) composite. *The International Journal of Advanced Manufacturing Technology, 134* (3)**,** pp.1563-1580.

[6] Przestacki, D., Szymanski, P. & Wojciechowski, S., 2016. Formation of surface layer in metal matrix composite a359/20sicp during laser-assisted turning. *Composites Part A: Applied Science and Manufacturing, 91***,** pp.370-379.

[7] Subramanyam, B. & Periyasamy, P., 2024. Microstructure &amp; mechanical properties evaluation of Al6082/AlSi10 Mg composite for light weight structural applications. *Mechanics of Advanced Composite Structures, 11* (2)**,** pp.309-320.

[8] Cho, H., Jun, Y. & Yang, M.-Y., 1993. Five-axis cnc milling for effective machining of sculptured surfaces. *The International Journal of Production Research, 31* (11)**,** pp.2559-2573.

[9] Nicholls, C.J., Boswell, B., Davies, I.J. & Islam, M.N., 2017. Review of machining metal matrix composites. *The International Journal of Advanced Manufacturing Technology, 90***,** pp.2429-2441.

[10] Lakshmanan, K., Pandian, P., Sivaprakasam, R. & Sundaram, K., 2025. Studies on progress of aluminum based composites for automotive applications and its damping characteristics – a review. *Mechanics of Advanced Composite Structures, 12* (1)**,** pp.25-42.

[11] Sougavabar, M.A., Niknam, S.A. & Davoodi, B., 2023. Experimental characterization of tool wear morphology in milling of al520-mmc reinforced with sic particles and additive elements bi and sn. *Journal of Materials Research and Technology, 24***,** pp.571-585.

[12] Steinbacher, L., Wegmann, T. & Freitag, M., 2024. Production control with reinforcement learning for a matrix-structured production system. *International Journal of Production Research***,** pp.1-23.

[13] Alipour Sougavabar, M., Niknam, S.A., Davoodi, B. & Songmene, V., 2022. Milling al520-mmc reinforced with sic particles and additive elements bi and sn. *Materials, 15* (4)**,** pp.1533.

[14] Lalmuan, S., Das, S., Chandrasekaran, M. & Tamang, S.K., 2017. Machining investigation on hybrid metal matrix composites-a review. *Materials Today: Proceedings, 4* (8)**,** pp.8167-8175.

[15] Fard, R.K., Afza, R.A. & Teimouri, R., 2013. Experimental investigation, intelligent modeling and multi-characteristics optimization of dry wedm process of al–sic metal matrix composite. *Journal of Manufacturing Processes, 15* (4)**,** pp.483-494.

[16] Bharat, N. & Bose, P., 2022. A study on conventional and non-conventional machining behaviour of metal matrix composites: A review. *International Journal of Ambient Energy, 43* (1)**,** pp.7600-7616.

[17] Bharat, N. & Bose, P., 2024. Effect of sic and tio2 nanoparticles on machinability of aa7178 metal matrix composite: A comparative analysis using taguchi and gra approaches. *JOM, 76* (6)**,** pp.2794-2806.

[18] Rodríguez, J., Garrido-Maneiro, M., Poza, P. & Gómez-Del Río, M., 2006. Determination of mechanical properties of aluminium matrix composites constituents. *Materials Science and Engineering: A, 437* (2)**,** pp.406-412.

[19] Palanikumar, K. & Karthikeyan, R., 2007. Assessment of factors influencing surface roughness on the machining of al/sic particulate composites. *Materials & design, 28* (5)**,** pp.1584-1591.

[20] Ozben, T., Kilickap, E. & Cakır, O., 2008. Investigation of mechanical and machinability properties of sic particle reinforced Al-MMC. *Journal of materials processing technology, 198* (1-3)**,** pp.220-225.

[21] Weng, Y., Ding, L., Zhang, Z., Jia, Z., Wen, B., Liu, Y., Muraishi, S., Li, Y. & Liu, Q., 2019. Effect of ag addition on the precipitation evolution and interfacial segregation for al–mg–si alloy. *Acta Materialia, 180***,** pp.301-316.

[22] Nordin, N.A., Farahany, S., Ourdjini, A., Bakar, T.a.A. & Hamzah, E., 2013. Refinement of mg2si reinforcement in a commercial al–20% mg2si in-situ composite with bismuth, antimony and strontium. *Materials Characterization, 86***,** pp.97-107.

[23] Angadi, S.B., Kumar, S., Nagaral, M., Auradi, V. & Valukula, B., 2025. Effect of ceramic boron carbide particles addition on the mechanical and microstructural characteristics of Al 7020 alloy composites. *Mechanics of Advanced Composite Structures, 12* (1)**,** pp.169-180.

[24] Laghari, R.A., Jamil, M., Laghari, A.A., Khan, A.M., Akhtar, S.S. & Mekid, S., 2023. A critical review on tool wear mechanism and surface integrity aspects of sicp/al mmcs during turning: Prospects and challenges. *The International Journal of Advanced Manufacturing Technology, 126* (7)**,** pp.2825-2862.

[25] Ciftci, I., 2009. Cutting tool wear mechanism when machining particulate reinforced mmcs. *Technology, 12* (4)**,** pp.275-282.

[26] Kannan, T., Srinivasan, T., Kumari, N.C.K., Mohankumar, M. & Sivaraj, S., 2025. *Modern machining of metal matrix composites. Fundamentals and advances in metal matrix composites.* CRC Press, pp.196-207.

[27] Gutierrez-Santillan, A., Figueroa, C.G., Reyes-Ruiz, C., Ortiz, A. & Schouwenaars, R., 2025. Influence of heat treatment on the wear behavior of an Al-Cu-Mg-Sn MMC reinforced with tib2. *Wear*, pp.205963.

[28] Chen, Z., Ding, F., Zhang, Z., Gu, D., Liao, Q., Chen, M. & Wang, B., 2024. The study on the effect of various tool wear indicators on the machining of mmcs. *Journal of Materials Research and Technology, 30*, pp.231-244.

[29] Sandhu, I.S., Maurya, S.K. & Manna, A., 2023. Experimental investigation on ecdm parameters during μ-drilling of fabricated Zn/(ag+ fe)-mmc for biodegradable application. *Journal of the Brazilian Society of Mechanical Sciences and Engineering, 45* (8)**,** pp.402.

[30] Sundaramoorthy, R. & Ravindran, R., 2019. Tool wear optimization in CNC milling operation of Al–Mg2Si alloys by taguchi method. *SN Applied Sciences, 1* (9)**,** pp.1093.

[31] Thilagham, K., Krishnamachary, P., Saravanakumar, S., Mahendran, A., Kaliappan, S., Soudagar, M.E.M., Kannan, S., Al Obaid, S. & Alharbi, S.A., 2025. Optimization of machining aa4015/b4c metal matrix composites by taguchi method. *Surface Review and Letters, 32* (02)**,** pp.2450108.

[32] Bharat, N., Bose, P., Kumar, V. & Mishra, V., 2025. Comparative study of supervised learning algorithm to predict cutting force and surface roughness during laser assisted turning of novel aa7178/ntio2 nanocomposite. *Optics & Laser Technology, 192*, pp.113430.

[33] Abellán-Nebot, J.V., Vila Pastor, C. & Siller, H.R., 2024. A review of the factors influencing surface roughness in machining and their impact on sustainability. *Sustainability, 16* (5)**,** pp.1917.

[34] Farahany, S., Ghandvar, H., Bozorg, M., Nordin, A., Ourdjini, A. & Hamzah, E., 2020. Role of sr on microstructure, mechanical properties, wear and corrosion behaviour of an al–mg2si–cu in-situ composite. *Materials Chemistry and Physics, 239*, pp.121954.

[35] Wu, X.-F., Zhang, G.-A. & Wu, F.-F., 2013. Influence of bi addition on microstructure and dry sliding wear behaviors of cast al-mg2si metal matrix composite. *Transactions of Nonferrous Metals Society of China, 23* (6)**,** pp.1532-1542.

[36] Chikkanna, A.K., Manjunath, K.V., Jayappa, K., Reddy, M. & Biradar, A., 2024. Effect of chilling &amp; b4c content on machining efficiency and surface quality in wire-cut machining of aluminum matrix chilled composites. *Mechanics of Advanced Composite Structures, 11* (2)**,** pp.341-350.

[37] Doluk, E., Rudawska, A. & Legutko, S., 2025. Effect of depth of cut and number of layers on the surface roughness and surface homogeneity after milling of al/cfrp stacks. *Materials, 18* (1)**,** pp.206.

[38] Prabhu, R. & Kanthababu, M., 2024. Prediction of surface roughness and depth of cut in abrasive waterjet milling of alumina ceramic using machine learning algorithms. *Expert Systems with Applications, 246*, pp.123168.

[39] Kumar P, K., Lokeshwar, G., Reddy, C.U.K., Jyotis, A., Shetty, S., Acharya, S. & Shetty, N., 2024. Effect of drilling parameters on surface roughness and delamination of ramie–bamboo-reinforced natural hybrid composites. *Journal of Manufacturing and Materials Processing, 8* (5)**,** pp.195.

[40] Pang, Z., Wang, S., Yin, X., Yu, S. & Du, N., 2022. Effect of spindle speed during ultrasonic rolling on surface integrity and fatigue performance of ti6al4v alloy. *International Journal of Fatigue, 159*, pp.106794.

[41] Al-Tameemi, H.A., Al-Dulaimi, T., Awe, M.O., Sharma, S., Pimenov, D.Y., Koklu, U. & Giasin, K., 2021. Evaluation of cutting-tool coating on the surface roughness and hole dimensional tolerances during drilling of al6061-t651 alloy. *Materials, 14* (7)**,** pp.1783.

[42] Davoodi, B. & Tazehkandi, A.H., 2014. Experimental investigation and

optimization of cutting parameters in dry and wet machining of aluminum alloy 5083 in order to remove cutting fluid. *Journal of Cleaner Production, 68,* pp.234-242.

[43] Das, M., Mishra, D. & Mahapatra, T.R., 2019. Machinability of metal matrix composites: A review. *Materials Today: Proceedings, 18,* pp.5373-5381.

[44] Aabid, A., Murtuza, M.A., Khan, S.A. & Baig, M., 2022. Optimization of dry sliding wear behavior of aluminium-based hybrid mmc's using experimental and doe methods. *journal of materials research and technology, 16,* pp.743-763.

[45] Ahmad, S., Tian, Y., Hashmi, A.W., Singh, R.K., Iqbal, F., Dangi, S., Alansari, A., Prakash, C. & Chan, C.K., 2024. Experimental studies on mechanical properties of al-7075/tio2 metal matrix composite and its tribological behaviour. *Journal of Materials Research and Technology, 30,* pp.8539-8552.

[46] Davim, J.P., 2001. A note on the determination of optimal cutting conditions for surface finish obtained in turning using design of experiments. *Journal of materials processing technology, 116* (2-3), pp.305-308.

[47] Bharat, N., Kumar, A. & Bose, P., 2022. A study on soft computing optimizing techniques. *Materials Today: Proceedings, 50,* pp.1193-1198.

[48] Jiang, B., Wang, H., Yi, D., Tian, Y., Shen, F., Wang, B., Liu, H. & Hu, Z., 2020. Effect of ag addition on the age hardening and precipitation behavior in an al-cu-li-mg-zn-mn-zr alloy. *Materials Characterization, 162,* pp.110184.

[49] Cetin, M.H. & Kilincarslan, S.K., 2020. Effects of cutting fluids with nano-silver and borax additives on milling performance of aluminium alloys. *Journal of Manufacturing Processes, 50,* pp.170-182.

[50] Bertolini, R., Andrea, G., Alagan, N.T. & Bruschi, S., 2023. Tool wear reduction in ultrasonic vibration-assisted turning of sic-reinforced metal-matrix composite. *Wear, 523,* pp.204785.

[51] Laghari, R.A., He, N., Jamil, M. & Gupta, M.K., 2023. Tribological and machining

characteristics of milling sicp/al mmc composites under sustainable cooling conditions. *The International Journal of Advanced Manufacturing Technology, 128* (5-6), pp.2613-2630.

[52] Sankhla, A.M., Patel, K.M., Makhesana, M.A., Saxena, K.K. & Gupta, N., 2022. Experimental investigation of tool wear in machining of sic based al-mmc. *Advances in Materials and Processing Technologies, 8* (sup2), pp.635-654.

[53] Bharat, N. & Bose, P., A study on machining behaviour of metal matrix composite: A review. International conference on energy, materials sciences & mechanical engineering, 2020. Springer, 367-374.

[54] Usca, Ü.A., Uzun, M., Şap, S., Kuntoğlu, M., Giasin, K., Pimenov, D.Y. & Wojciechowski, S., 2022. Tool wear, surface roughness, cutting temperature and chips morphology evaluation of al/tin coated carbide cutting tools in milling of cu−b−crc based ceramic matrix composites. *journal of materials research and technology, 16,* pp.1243-1259.

[55] Bharat, N. & Bose, P., 2021. An overview on machinability of hard to cut materials using laser assisted machining. *Materials Today: Proceedings, 43,* pp.665-672.

[56] Singh, S., Kaushal, S. & Forzan, M., 2022. *Materials system for functional properties of metal matrix composites: Self-lubricating, anti-wear, and self-cleaning properties. Metal matrix composites.* CRC press, pp.1-26.

[57] Valizade, N. & Farhat, Z., 2024. A review on abrasive wear of aluminum composites: Mechanisms and influencing factors. *Journal of Composites Science, 8* (4), pp.149.

[58] Bharat, N. & Bose, P., 2025. Predictive modeling of cutting forces in laser-assisted turning of aa7178-nano sic composite using different backpropagation neural networks. *Measurement, 245,* pp.116673.

[59] Gassour, H., El-Magd, G.E.-D.a.A., Mazen, A. & Ibrahim, A.M.M., 2023. Characterization of aluminum composite reinforced by silver nanoparticles. *Scientific reports, 13* (1), pp.17952.